Escherichia coli cAMP Receptor Protein−DNA Complexes. 2. Structural Asymmetry of DNA Bending†

Erica A. Pyles‡ and J. Ching Lee*

Department of Human Biological Chemistry and Genetics, The University of Texas Medical Branch, Galveston, Texas 77555-1055

Received October 2, 1997; Revised Manuscript Received January 23, 1998

ABSTRACT: The effect of DNA sequence variability and the degree of cyclic AMP receptor protein (CRP)-induced bending of the flanking ends of fluorescently labeled DNA were investigated by steady-state fluorescence and differential phase polarization studies in the presence and absence of CRP. Six sequences, including the primary CRP binding sites of *lac P1* (class I) and *gal P1* (class II), were studied. Excitation and emission spectra of CPM−DNA upon binding CRP were observed to be qualitatively similar to one another, regardless of the CRP binding site sequence examined or the location of the probe. This result implies that the probe is not interacting with the protein. However, the magnitude of the changes in the fluorescence intensities of sensitized emission spectra of CPM−DNA is apparently dependent on the DNA sequence, indicating that the environments of the flanking ends of DNA may be different from one another in the protein−DNA complex. Differential phase polarization results were qualitatively consistent with the fluorescence energy transfer measurements. The implication of this study supports the idea that the DNA is bent symmetrically in the *lac*−CRP complex but is asymmetrically bent in the *gal*−CRP complex. The sequence in the half-site in conjunction with the flanking sequence defines the geometry of the bent DNA. It appears that the CRP-induced bend in the DNA may also be class dependent. This may be an important feature used by the system to regulate transcription at different promoter sites.

Structural asymmetry apparently plays a functional role in the activity of CRP,[1] since the asymmetric CRP−$cAMP_1$ molecule but not CRP−$cAMP_2$ binds with high affinity to specific DNA in vitro (*1*, *2*). No sequence has been found yet to bind with high specificity to free CRP or CRP−$cAMP_2$. Another feature of structural asymmetry may be related to the structure of DNA when bound to proteins.

A common feature found in many DNA binding proteins, including CRP, is that the protein distorts the DNA structure when it binds to the DNA (*3*−*6*). Evidence for the CRP-induced DNA bending has been shown in electrophoretic studies (*7*−*9*), the cocrystal structure of the CRP−DNA complex (*10*), and fluorescence studies (*11*). The fluorescence results show that, although the active CRP conformation of CRP−$cAMP_1$ and the DNA sequence of *lac* are asymmetric, the bending of the two ends of the DNA by CRP is symmetric in nature (*11*). However, the extent of symmetry of the CRP-induced bend in DNA may not be the same for all CRP binding sites. Ebright and co-workers demonstrated that the properties of the CRP mutants in association with DNA and RNA polymerase (*12*−*14*) differ depending on the class of the CRP binding site. These CRP mutants may be reflecting structural (dynamic) differences between CRP−*gal* (class II) and CRP−*lac* (class I) complexes, although differences between CRP−*gal* and CRP−*lac* are not detected by DNase I (*15*, *16*) and hydroxyl radical footprinting experiments (*17*). It is possible that under those experimental conditions these specific footprinting studies are not capable of detecting the differences in the CRP-induced structural changes in DNA brought about by the specific interaction of the protein with the DNA. A consequence of the ability of CRP to introduce distinct degrees of DNA deformation in a CRP binding site is that it may provide a different set of contact points between RNA polymerase and CRP. It has been proposed that the mechanisms of transcriptional control by CRP differ, and the topology of the protein−DNA complex differs from class to class (*18*). The principal interaction of CRP with class III promoter sites induces structural alterations of the DNA to allow transcriptional factor proteins that bind to distal sites on DNA to be spatially proximal to one another (i.e. *malT* promoter; *19*). There is also evidence to support the hypothesis that different protein contacts between RNA polymerase and CRP exist when the proteins are associated to class I (i.e. *lac* promoter) and class II (i.e. *gal* promoter) CRP binding sites on DNA. Recent studies using CRP mutated in a flexible loop region (amino acids located between 156 and 164) implicate this region's importance in establishing effective communication between RNA poly-

† Supported by NIH Grant GM45579 and Robert A. Welch Foundation Grants H-0013 and H-1238. The Laboratory for Fluorescence Dynamics at the University of Illinois at Urbana−Champaign (UIUC) is supported jointly by NIH Grant RR 03155 and UIUC.

* To whom correspondence should be addressed.

‡ Present address: Chemistry Department, Rollins College, Winter Park, FL 32789-4499.

[1] Abbreviations: CRP, cAMP receptor protein; TEDKG buffer, 50 mM Tris, 1 mM K_2EDTA, 1 mM DTT, 100 mM KCl, and 10% (w/v) glycerol at pH 7.80 and 25 °C; TEK(100) buffer, 50 mM Tris, 1 mM K_2EDTA, and 100 mM KCl at pH 7.8 and 25 °C; TEK(75) buffer, 50 mM Tris, 1 mM K_2EDTA, and 75 mM KCl at pH 7.80 and 25 °C; TE buffer, 50 mM Tris and 1 mM K_2EDTA at pH 7.80 and 25 °C.

S0006-2960(97)02451-3 CCC: $15.00
Published on Web 03/21/1998

merase and the CRP−DNA complex for both class I and II promoters (*12*−*14*, *20*). Amino acid substitutions and deletions in the α subunit of RNA polymerase located at amino acid positions 258−265 interfered with transcriptional activation of class I promoter sites but did not affect the transcription processes for class II promoter sites. Thus, it was proposed that RNA polymerase is capable of distinguishing the difference between class I and class II promoter sites by making a different set of contacts between CRP and RNA polymerase in the presence of the promoter site. This may be a consequence of different degrees of DNA bending induced by CRP. Thus, the contribution of DNA sequence asymmetry to the energetics of specific CRP−DNA recognition (*21*) and the topology of bent DNA is investigated.

The effect of the DNA sequence asymmetry on the dynamic properties of specific CRP−DNA complexes was examined. These properties were investigated using steady-state fluorescence and differential phase polarization studies of fluorescently labeled CRP binding sites in the presence and absence of CRP. The flanking ends of *lac* and *gallac* (a hybrid sequence of *gal* and *lac*) in the presence of CRP are similar to one another, i.e. symmetric DNA bending. However, the ends of *gal* in the protein−DNA complex are bent asymmetrically.

MATERIALS AND METHODS

CRP and double-stranded (ds) DNA sample preparations are described in ref *11* and in the preceding paper (*21*).

Lifetime and Rotational Correlation Times. Lifetime and differential phase polarization measurements were performed at the Laboratory of Fluorescence Dynamics at the University of Illinois. A Nd:YAG laser pumping DCM dye was tuned to 350 nm, and emission was observed beyond 440 nm by placing Schott KV 399 and Hoya Y44 cutoff filters in the emission path. A 4 × 10 mm quartz fluorescence cell was used, and the excitation beam passed through the longer path. POPOP [1,4-bis(phenyloxazol-2-yl)benzene] in ethanol was used as a standard reference (τ_f = 1.35 ns; *22*). Measurements were conducted on solutions containing CPM−DNA (800 nM) and cAMP (150 μM) in the presence and absence of CRP (1 μM) in TEK(75) at pH 7.8 and 25 °C, in which the K_{app} of CRP−DNA formation was at least 20-fold higher than that in TEK(100). Lifetime and differential phase polarization data were collected at least twice for each solution. Errors are expressed in terms of 67% confidence intervals. Data analyses were performed at the Laboratory of Fluorescence Dynamics.

Energy Transfer Measurements. Steady-state excitation and emission spectra were recorded in the ratio mode using a SLM 8000C instrument equipped with Glan-Thompson calcite prism polarizers, an enhanced sensitivity cell holder, photon counting detection, and a circulating water bath at 25.0 ± 0.1 °C. Both excitation and emission polarizers were set to "magic angles" to eliminate polarization effects (*23*). Excitation spectra were corrected by a rhodamine solution in the reference channel, and the emission spectra are uncorrected. A 2 × 10 mm quartz fluorescence cell was used, and it was oriented so the excitation beam passed through the longer path. The excitation wavelength for emission spectra of CPM−DNA was 295 nm, and the emission wavelength ranged from 310 to 580 nm. For excitation spectra of CPM−DNA, the emission wavelength was 500 nm and the excitation wavelength ranged from 270 to 450 nm. Data were collected in 2 nm intervals. The buffer was TEK(75) at pH 7.8 and 25 °C. Concentrations of DNA and protein were designed to ensure stoichiometric binding of the DNA to CRP. Previous experiments have examined the effect of high concentrations of CRP binding sites and CRP on the stoichiometry of the CRP−DNA complex (*1*, *2*). Under both high (∼800 nM) and low (∼20 to 200 nM) concentrations of DNA, the stoichiometry of the complex was measured to be 1:1. In each titration, the observed anisotropy remained constant after 1:1 complex formation. In addition, the total change in anisotropy was similar to those obtained from equilibrium measurements, and also well below the limiting anisotropy of the probe. This indicates that DNA−protein aggregation is negligible. CRP does not self-associate in the presence or absence of cAMP (unpublished data). Thus, aggregation of CRP or CRP−DNA complex most likely does not occur under the experimental conditions employed. Spectra of CPM−DNA [*gal* (*GCGG*),[2] *gallac* (*GCLG*), *lac* (*LCLL*), and *ranlac* (*RCLR*) at 800 nM and *lac* and *gallac* (*GCLG*), *galicapx* (*GCCG*), and *lacx* (*LCLLX*) at 200 nM] in the presence of cAMP (150 μM) were recorded. Subsequently, CRP was added to the CPM−DNA solution and the solution gently mixed, and the solution was allowed to attain equilibrium before spectra were recorded. The final concentration of CRP added to solutions containing *gal*, *GCLG*, *LCLL*, and *RCLR* was 970 nM. The final concentration of protein added to solutions containing *LCLL*, *LCLLX*, *GCLG*, or *GCCG* was 240 nM. Concentrations of solutions employed were chosen to avoid complications of inner filter effect. Solutions were gently mixed by inversion and incubated for several minutes to ensure temperature equilibration, and spectra were recorded. Mixing the solutions by gentle stirring or inversion yielded the same results. CRP binding to *GCLG* and *LCLL* sequences at both concentrations produced similar results. Each solution containing fluorophore was run at least three times. Spectra of buffer solutions were also collected and were subtracted from the appropriate fluorophore's spectrum. Spectra of DNA−protein complexes were corrected for the dilution incurred upon the addition of CRP to CPM−DNA (<5% volume change). Data are represented in terms of the percent change in fluorescent intensities observed at the excitation and emission maxima of the CPM−DNA−CRP complex relative to those observed for free CPM−DNA. A change in fluorescent intensity of CPM−DNA in the presence of CRP is represented by a positive or negative percentage change. Furthermore, an apparent measure of fluorescence resonance energy transfer was calculated using the sensitized emission spectral intensities. The ratio of the integrated fluorescence intensity (278 nm to 288 nm) of CPM−DNA (fluorophore located proximal to the TGTGA motif) in the presence and absence of CRP was calculated as an apparent measure of fluorescence resonance energy transfer as previously described (*11*). The integrated intensi-

[2] Using the nomenclature system adopted in the preceding paper. The four-letter code denotes the flanking sequence proximal to the conserved TGTGA half-site, the conserved half-site, the variable half-site, and the flanking sequence. In this nomenclature system, the letters and their sequence origins are as follows: C, conserved TGTGA; G, *gal*; L, *lac*; and R, random. See Figure 1 of Pyles et al. (*21*).

Table 1: Association Constants for CRP−DNA Complexes[a]

CRP binding site	sequence[b]	K_{app} x 10^{-6} (M^{-1})[c]
lac PI (*LCLL*) →	ATTAA**TGTGA**GTTAGC**TCACT**CATTA	41 (35, 49)[d,e]
lacx PI (*LCLLX*) →	XATTAA**TGTGA**GTTAGC**TCACT**CATTA[f]	54 (39, 74)[g]
gal PI (*GCGG*) ←	AAAAG**TGTGA**CATGGA**ATAAA**TTAGT	9.5 (8.5, 11)[d]
gallac (*GCLG*)	AAAAG**TGTGA**CATGGA**TCACT**TTAGT	160 (130, 200)[d]
GALICAPX (*GCCG*)	XAAAAG**TGTGA**CATGGA**TCACA**TTAGT	2500 (960, 17100)[g]
RANLAC (*RCLR*)	CTCAG**TGTGA**ATACCA**TCACT**CCCAG	5.3 (4.4, 6.2)[g]

[a] Measured in TEK(100) in the presence of 150 μM cAMP at pH 7.80 and 25.0 °C. [b] Sequences are listed from the 5′-end to the 3′-end. The recognition half-sites are bold. Arrows represent the direction of transcription. [c] Apparent equilibrium constants of CRP binding to DNA were calculated from eq 3 in Materials and Methods in the preceding paper (*21*). [d] From ref *2*. [e] Errors in parentheses are expressed in terms of 75% confidence intervals. [f] The letter X represents the thiol linker covalently attached to the 5′-end via conventional solid support chemistry. [g] From the preceding paper (*21*).

ties were corrected for a change in CPM fluorescence induced by CRP binding to DNA when CPM−DNA was excited above 320 nm (i.e. where protein fluorescence is negligible).

Fluorescence resonance energy transfer was performed on DNA that was doubly labeled with two fluorophores, CPM and FM, with each fluorophore located at opposite ends (attached at the 5′-ends) of the dsDNA. A doubly labeled DNA is designated CPM−DNA−FM. To ensure that the signal changes observed are solely due to Förster energy, both steady-state emission intensities and lifetimes were measured. These data were used to calculate the efficiency of energy transfer by employing the relation $E = 1 - F_{da}/F_d = \tau_{da}/\tau_d$ (*24*, *25*). E, F_{da}, and τ_{da} are the efficiency of fluorescence resonance energy transfer, fluorescence intensity, and fluorescence lifetime of the donor in the presence of the acceptor, respectively. F_d and τ_d are the fluorescence intensity and fluorescence lifetime of the donor, respectively. Steady-state spectra of CPM−DNA−FM (*GCGG*, *GCLG*, and *LCLL*) were recorded in the presence and absence of CRP in TEK(75) and 150 μM cAMP at pH 7.8 and 25.0 °C, as described above. Spectral data (excitation and emission spectra) and lifetime measurements yielded similar results, indicating fluorescence resonance energy transfer was the sole photophysical process occurring for CPM−DNA−FM. For excitation spectra, the emission wavelength was 520 nm and the excitation wavelength ranged from 270 to 515 nm. For emission spectra, the excitation wavelengths were 390 and 460 nm, and the emission ranged from 400 to 650 nm and 465 to 650 nm, respectively. Stoichiometric concentrations of CRP and CPM−DNA−FM in TEK(75) containing 150 μM cAMP at pH 7.8 were used as described above. Each spectrum or lifetime was measured at least twice for each sample. The efficiency of energy transfer from the donor (CPM) to the acceptor (FM) on DNA was calculated from corrected, relative fluorescence intensity from the emission spectrum at 475 nm in the presence and absence of the protein. The emission intensity of the DNA−protein complex was corrected for the contribution of fluorescein's (acceptor) emission since the emission spectra of the donor (CPM) and acceptor (FM) overlap. The emission spectra were measured with two different excitation wavelengths (λ_{ex} = 390 nm and λ_{ex} = 460 nm). Excitation of the sample at 460 nm yields a spectrum of only the acceptor fluorescence. The emission spectra collected at two different excitation wavelengths were normalized so that the intensities at 520 nm were equal. The fluorescence of the normalized fluorescein spectrum was subtracted from the normalized CPM−DNA−FM spectrum to account for the contribution of the fluorescence of the acceptor to the emission spectrum of the donor (*26*). In addition, the fluorescence of CPM−DNA was measured and the spectrum was corrected for the incomplete labeling efficiency of the DNA and also normalized. The fluorescence intensities at 475 nm for the DNA in the presence and absence of CRP were used to calculate the efficiency of energy transferred from CPM to FM on DNA in the presence and absence of CRP. In addition, the lifetimes of CPM−*gal*−FM, CPM−*GCLG*−FM, and CPM−DNA under the same solution conditions described above were measured in the presence and absence of CRP with the excitation polarizer set to 36° and an interference filter (475 nm) placed in the emission path. The emission polarizer was removed. Data were fit to two lifetimes. One lifetime corresponded to the lifetime of CPM-labeled DNA. The other lifetime was very short (<0.25 ns) and contributed ∼5% to the total signal. No lifetime characteristic of free fluorescein was detected (τ_f = 4.0 ns; *27*). A weighted average of the lifetimes [$\langle\tau\rangle = \sum(\text{fxb})_i\tau_i$] was used to calculate the efficiency of energy transfer.

Similar efficiencies of energy transfer were obtained using either steady-state spectra or lifetime measurements. Using multiple methods to monitor the same process increases the reliability of the data even if the energy transfer observed is small (*24*, *25*). Further precautions were taken to ensure that observations were not due to one preparation of fluorescently labeled DNA. Different preparations of CRP and labeled DNA were used. In addition, the labeling of DNA was performed on DNA synthesized at different times.

RESULTS

Symmetry of DNA Bending. Information such as the symmetry of bending of the DNA in the presence of CRP was obtained by measuring fluorescence resonance energy transfer from emission and sensitized emission spectra, to ensure that the spectral changes observed were due to Förster nonradiative energy (*24*, *25*, *28*). DNA sequences were labeled with the fluorophore CPM located at the 5′-ends of the two strands of the DNA containing CRP binding sites as listed in Table 1. Previous studies have demonstrated that there is good spectral overlap between the emission spectrum of the donor tryptophan residues in CRP and the absorption spectrum of the acceptor CPM (*11*). This is one criterion needed to measure fluorescence resonance energy transfer from the protein to CPM−DNA. Therefore, labeling the DNA on one end or the other will provide information about the apparent efficiency of energy transfer from the protein to the two ends of CPM−DNA and, thus, the

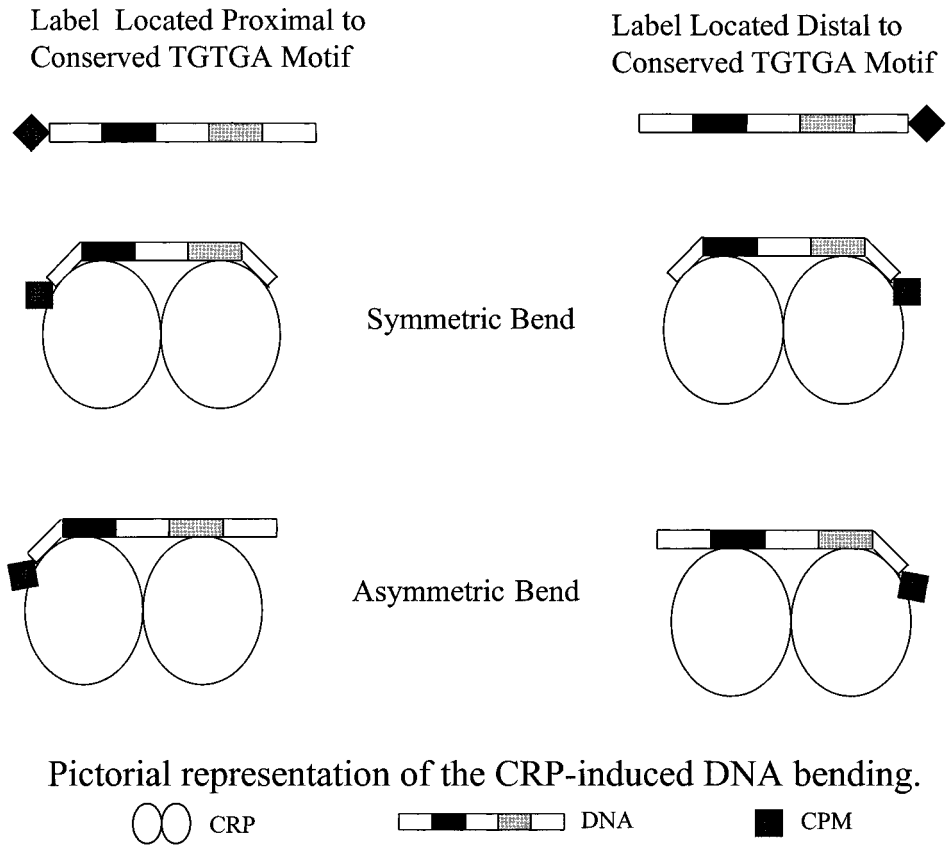

FIGURE 1: Pictorial representation of CRP-induced DNA bending. The conserved TGTGA and inverted repeat sequences are shown in dark and light gray rectangles, respectively. In theory, one would expect similar efficiencies in fluorescence resonance energy transfer from either end of the DNA if the DNA is bent symmetrically when it is bound to CRP. However, one would expect a difference in the efficiencies of energy transfer if the DNA was bent asymmetrically when it is bound to CRP.

symmetry of the CRP-induced bend in DNA. Figure 1 depicts a cartoon of the two possible modes of CRP-induced bending of the DNA. The spectral properties of CPM−DNA when complexed to CRP would be the same if CRP induces a symmetrical bend in the DNA, regardless of the DNA sequence and location of CPM. In contrast, if CRP binding to the DNA results in an asymmetrical bend, then the spectral properties would be dependent on the location of the fluorescent probe.

Emission Spectra. The emission spectra of CPM−DNA contain an emission maximum at 480 nm which is characteristic of this fluorophore, CPM, in aqueous solution (*29*). The maximum and its fluorescence intensity were not perturbed by DNA sequence variation or the addition of protein when excited at 390 nm in most cases. These results imply that there is no interaction between the probe and protein. Any change in the fluorescence signal is a reflection of the location of the probe. CRP binding to CPM−DNA did affect the fluorescence intensity of the emission spectra of CPM−DNA when the solution was excited at 295 nm; thus, there was energy transfer from the tryptophan residues in CRP to CPM. As a representative example, the emission spectra of proximally and distally labeled[3] CPM−*GCLG* in the presence and absence of CRP are depicted in Figure 2. In the presence of cAMP, DNA binding to CRP results in a reduction in fluorescence intensity of the donor tryptophan residues in CRP (maximum at 345 nm) with a concomitant enhancement of fluorescence intensity of the acceptor's emission, CPM−DNA (maximum at 480 nm). The changes in the fluorescence intensity observed at 480 nm when CRP binds to CRP binding sites relative to that observed for free CPM−DNA are listed in Table 2. With the exception of distally labeled CPM−*GCGG*−CRP and both proximally and distally labeled CPM−*RCLR*−CRP complexes, an increase in fluorescence intensity of the DNA was observed in the presence of CRP. These results imply that, with the exceptions of those ends noted above, formation of the DNA−CRP complex causes all ends of DNA sequences tested to assume a shorter distance between the DNA ends and CRP; i.e. they all bend toward CRP. In contrast, the distal end of *GCGG* and both ends of *RCLR* do not bend or bend much less toward CRP.

Sensitized Emission Spectra. Excitation spectra of *LCLL*, *GCGG*, *GCLG*, *GCCG*, and *RCLR* in the presence and absence of CRP were measured in 150 μM cAMP (λ_{em} = 500 nm). As an example, spectra of proximally and distally labeled CPM−*GCLG* in the presence and absence of CRP are shown in Figure 3. Two maxima were observed in the excitation spectrum of CPM−DNA and are located at 285 and 396 nm. These wavelength maxima were found to be independent of DNA sequence and the presence of CRP. The addition of CRP to the CPM-labeled DNA resulted in an enhancement of fluorescence intensity at the 285 nm excitation band (Table 2). For any given CRP−DNA complex, with the exception of *LCLLX*−CRP, the magnitude of the change in the fluorescence intensity at 285 nm was

[3] The reference position is the conserved TGTGA motif, i.e. C in the four-letter code.

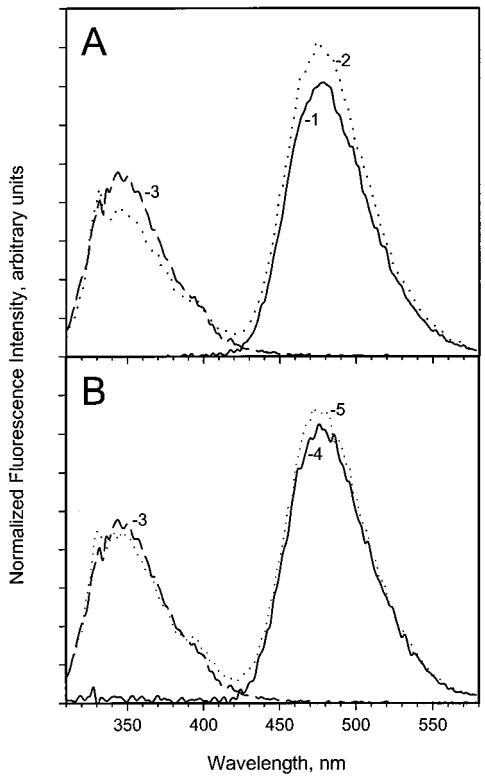

FIGURE 2: Emission spectra of CPM−*GCLG* in the presence and absence of CRP in TEK(75) containing 150 μM cAMP at pH 7.80 and 25.0 °C. DNA−protein complexes were prepared as described in Materials and Methods. The spectra of CPM−*GCLG* in the absence of CRP were normalized at 500 nm, and the appropriate factor was used to normalize their respective spectra recorded in the presence of CRP. (A) Spectra of proximally labeled CPM−*GCLG* in the presence (2, dotted curve) and absence (1, solid curve) of CRP. The emission spectrum of CRP is also shown (3, dashed curve). (B) Spectra of distally labeled CPM−*GCLG* in the presence (5, dotted curve) and absence (4, solid curve) of CRP. The emission spectrum of CRP is also shown (3, dashed curve).

always greater when the CPM fluorophore was covalently attached in a position proximal to the TGTGA motif, relative to that observed for CRP bound to the same DNA with the fluorescent label distal to the TGTGA motif. The magnitudes of the observed fluorescence enhancements are within statistical error of each other when CRP binds to DNA labeled with CPM.

An increase in fluorescence intensity in the excitation spectrum of CPM−DNA at the high-energy band located at 285 nm is expected if fluorescence resonance energy transfer is occurring, i.e. the energy of the tryptophans in the protein is being transferred to the fluorophore attached to DNA. Essentially no change in fluorescence intensities at the low-energy band located at 396 nm was observed for CRP binding to distally labeled CPM−*LCLL* and proximally labeled CPM−*GCGG*, *LCLL*, *LCLLX*, *GCLG*, *GCCG*, and *RCLR* (Figure 3 and column 4 of Table 2). For these CPM-labeled DNA, the excitation and emission spectra demonstrate that fluorescence resonance energy transfer does occur between the protein and CPM−DNA. In contrast, the low-energy band (396 nm) in the excitation spectrum of distally labeled CPM−*LCLLX*, *GCGG*, *GCLG*, *GCCG*, and *RCLR* is slightly quenched by CRP−DNA complex formation (Figure 3 and column 4 of Table 2). Quenching of the fluorescence intensity at the 396 nm band of the sensitized emission spectrum indicates that changes in the observed fluorescence signal are not solely governed by Förster nonradiative energy transfer in some CPM−DNA−CRP complexes (*24*, *28*).

The apparent efficiency of energy transfer from the protein to the probe in a position proximal to the conserved half-site (TGTGA motif) is essentially the same for *lac* (*LCLL*), *gal* (*GCGG*), *GCLG*, and *RCLR*. Nevertheless, the two CPM−DNA sequences which contain a longer spacer between the fluorophore and DNA have statistically different values for the apparent energy transfer (proximally labeled CPM−*LCLLX* and *GCCG*). The apparent energy transfer observed between CRP and *GCCG* is greater than that observed between CRP and the *LCLLX* sequence. Thus, the distance of the proximally labeled CPM−*GCCG* end is closer to that of the protein than to that of CPM−*LCLLX*. These results suggest that the degree of the CRP-induced bend in DNA is probably influenced by the sequences flanking the recognition motifs in the DNA. These results are consistent with information concerning the effect of the DNA sequence located outside of the recognition motifs on the CRP-induced bending in DNA examined by other methods (*30*).

Effect of the DNA Sequence on the Extent of CRP-Induced Bend in DNA. The steady-state excitation and emission spectra of CRP−DNA complexes infer that the ends of the CRP binding site on DNA reside in different environments, and the degree of bending may differ depending on the DNA sequence. Previous studies have shown that fluorescence resonance energy transfer of *lac* labeled with a donor (CPM) and acceptor (FM) located at 5′-ends of the DNA increases by ∼6 to 8% when the DNA is bound to CRP (*11*). It was also shown that there was very little energy transfer occurring between this donor−acceptor pair for the *lac* promoter site in the absence of CRP (∼1%). To examine if the overall degree of DNA bending induced by binding the protein is sequence dependent, fluorescence resonance energy transfer experiments were performed on doubly labeled *GCGG* and *GCLG* that were labeled at the 5′-ends of both strands with two different probes, CPM and FM. Similar efficiencies of energy transfer were obtained for CPM−*GCLG*−FM and CPM−*GCGG*−FM in the absence of CRP (<1%). A small increase in the efficiencies of energy transfer was observed (2.5%) when CPM−*GCGG*−FM and CPM−*GCLG*−FM were complexed to CRP relative to the efficiency of energy transfer observed for CPM−*LCLL*−FM bound to CRP (data not shown). Efficiencies of energy transfer calculated from the steady-state emission spectra of CPM−*GCGG*−FM and CPM−*GCLG*−FM in the presence of CRP are in good agreement with the values determined from lifetime measurements (data not shown). From the efficiency of energy transfer between the donor−acceptor pair on DNA, the distances between the ends of *GCGG* and *GCLG* were calculated. These calculations yielded a small decrease in distance between the donor−acceptor pair on *GCGG* and *GCLG*, from 100 to ∼90 Å when the DNA was complexed to CRP. Previous calculations estimate the distance between the donor−acceptor pair (CPM and FM) on *lac* decreases from 100 to 75−79 Å upon association of CRP with the DNA in the presence of cAMP (*11*). These results suggest that the CRP-induced bend in *GCLG* and *GCGG* may possibly be less than that observed for the *LCLL*−CRP complex. However, differences of only a few percentages in efficiency of energy transfer are usually difficult to

Table 2: Steady-State Fluorescent Properties of CRP−DNA Complexes[a]

DNA−CRP complex	probe[b] position	excitation maximum[c,d] 285 nm	excitation maximum[c,d] 396 nm	emission maximum[c,e] 480 nm	E_{app}[f]
lac−CRP or *LCLL*−CRP →	proximal	13.4 (4.7)[g]	−1.0 (4.0)	8.4 (2.2)	1.154 (0.046)
	distal	10.4 (1.5)	−2.2 (4.0)	8.8 (1.7)	
gal−CRP or *GCGG*−CRPT ←	proximal	10.8 (3.7)	−5.5 (4.5)	16.0 (2.2)	1.162 (0.064)
	distal	5.9 (3.0)	−3.9 (0.8)	0.3 (0.3)	
GCLG−CRP	proximal	21.4 (3.7)	0.3 (2.0)	9.6 (4.7)	1.141 (0.030)
	distal	8.2 (5.0)	−12.2 (4.0)	4.5 (1.3)	
lacx−CRP or *LCLLX*−CRP	proximal	11.6 (4.0)	−2.0 (2.8)	9.5 (0.6)	1.082 (0.043)
	distal	12.4 (2.7)	−5.2 (0.6)	8.1 (2.5)	
GCCGX−CRP	proximal	20.0 (6.0)	−2.8 (3.0)	2.7 (1.7)	1.209 (0.019)
	distal	11.7 (3.3)	−4.9 (0.4)	4.3 (0.6)	
RCLR−CRP	proximal	6.8 (5.9)	1.8 (2.5)	3.5 (5.0)	1.169
	distal	3.6 (1.8)	−8.8 (4.3)	0	

[a] Measured in TEK(75) and 150 μM cAMP at pH 7.80 and 25.0 °C. [b] CPM is covalently attached to the 5′-end of either strand. The reference position is the conserved TGTGA motif. Arrows indicate the direction of transcription. [c] Change in intensity between CPM−DNA in the presence and absence of CRP is represented in percent. Positive values indicate an increase in the fluorescence intensity of CPM−DNA in the presence of CRP relative to that of free CPM−DNA, while negative values reflect a quenching of CPM−DNA upon addition of CRP. [d] Emission wavelength was 500 nm. [e] Excitation wavelength was 295 nm. [f] Apparent energy transfer calculated from sensitized emission spectra. [g] Standard deviation in parentheses.

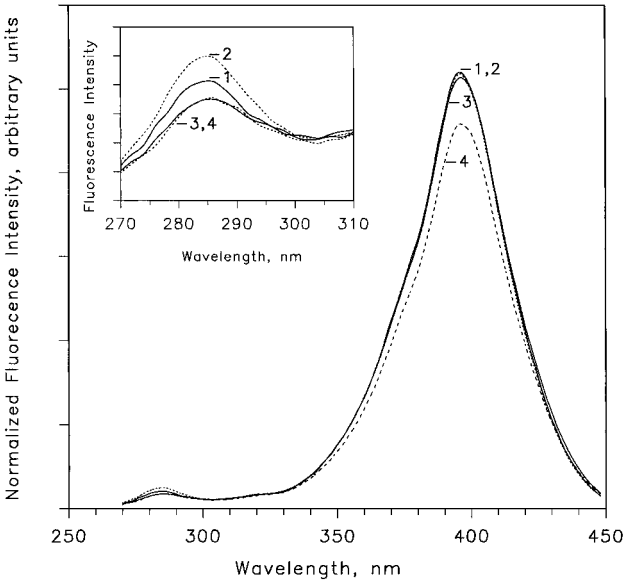

FIGURE 3: Excitation spectra of CPM−*GCLG* in the presence and absence of CRP in TEK(75) buffer containing 150 μM cAMP at pH 7.80 and 25.0 °C. DNA−protein complexes were prepared as described in Materials and Methods. Emissions of CPM−*GCLG* with the label located on the proximal and distal ends in the absence of CRP are depicted by curves 1 and 3 (solid curves), respectively. Spectra of CPM−*GCLG* with the label on the proximal and distal ends in the presence of CRP are represented by curves 2 and 4 (dashed curves), respectively. The emission wavelength was 500 nm. The spectra of CPM−*GCLG* in the absence of CRP were normalized at 400 nm, and the appropriate factor was used to normalize their respective spectra recorded in the presence of CRP.

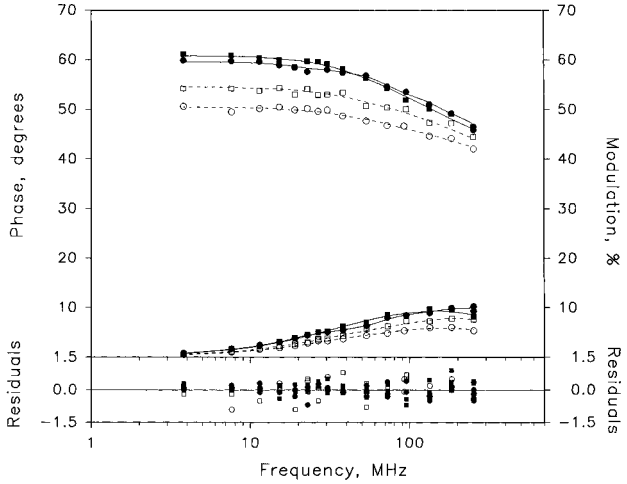

FIGURE 4: Multifrequency differential phase and modulation ratio data of *GCLG* in the presence and absence of CRP in TEK(75) buffer containing 150 μM cAMP at pH 7.80 and 25.0 °C. DNA−protein complexes were prepared as described in Materials and Methods. CPM was located at the proximal and distal ends of *GCLG* in the absence of CRP, and data are represented by the solid circles and squares (● and ■), respectively. The solid curves represent the best fit of the data. Open symbols (○ and □) represent proximally and distally labeled CPM−*GCLG*, respectively, in the presence of CRP, and the dashed curves represent the best fit of the data. The goodness of fits was judged by the value of χ^2 and the random distribution of the residuals about zero.

measure, and one should be cautious in using these data alone to determine the extent of CRP-induced deformation as a function of DNA sequence.

Effect of the DNA Sequence on the Dynamics of CRP−DNA Complexes. The spectral data of CPM−DNA suggest that there are small differences in the environment of the ends of the DNA when it is bound to CRP. Further information about the structural dynamics and environment of the flanking ends of CRP binding sites may be detected by measuring differential phase polarization of CPM−DNA in the presence and absence of the protein. A single lifetime of CPM−DNA was observed (τ_f = 3.619 ± 0.039 ns) for proximally labeled CPM−*LCLL*, *GCGG*, and *GCLG* and distally labeled CPM−*GCGG* and *GCLG* (data not shown). The distally labeled CPM−*LCLL* sequence also displayed a single lifetime, but its value was slightly higher (τ_f = 3.872 ± 0.042 ns) than that of CPM attached to the other sequences. The lifetime of free CPM−DNA was found to be insensitive to protein, but decreases in the phase and modulation ratio of CPM−*LCLL*, CPM−*GCLG*, and CPM−*GCGG* were observed upon CRP binding to the DNA. As a representative, typical data set for phase and modulation ratios of CPM−DNA, the graph for CPM−*GCLG* in the presence and absence of CRP is depicted in Figure 4. The fluorophore is able to detect differences in its environment because the phase and modulation ratio of proximally labeled CPM−*GCGG* and CPM−*GCLG* are more perturbed by the

Table 3: Rotational Correlation Times of CPM−DNA in the Presence and Absence of CRP[a]

sample	probe[b] position	r_o[c]	fxb_2[d]	ϕ_1[e] (ns)	ϕ_2[f] (ns)	χ_r^2[g]
lac (*LCLL*)	proximal	0.336 (0.320, 0.344)[h]	0.651 (0.617, 0.677)	0.742 (0.586, 0.914)	8.95 (8.06, 10.2)	1.19
	distal	0.354 (0.345, 0.366)	0.655 (0.638, 0.670)	0.558 (0.436, 0.691)	9.19 (8.46, 10.1)	1.23
gal (*GCGG*)	proximal	0.340 (0.333, 0.348)	0.630 (0.492, 0.662)	0.854 (0.684, 1.04)	10.6 (9.35, 12.5)	1.49
	distal	0.338 (0.332, 0.346)	0.642 (0.613, 0.667)	0.769 (0.628, 0.926)	9.49 (8.58, 10.7)	1.05
gallac (*GCLG*)	proximal	0.343 (0.334, 0.359)	0.665 (0.626, 0.693)	0.702 (0.495, 0.936)	9.47 (8.31, 11.2)	2.94
	distal	0.337 (0.325, 0.362)	0.656 (0.601, 0.692)	0.682 (0.411, 0.992)	9.00 (7.60, 11.3)	3.71
lac−CRP or *LCLL*−CRP	proximal	0.340 (0.335, 0.346)	0.713 (0.690, 0.731)	0.857 (0.701, 1.03)	20.9 (18.2, 24.7)	0.969
	distal	0.343 (0.336, 0.351)	0.706 (0.686, 0.722)	0.749 (0.593, 0.918)	20.9 (18.0, 24.6)	1.42
gal−CRP or *GCGG*−CRP	proximal	0.336 (0.331, 0.340)	0.732 (0.707, 0.753)	1.02 (0.844, 1.22)	25.2 (21.7, 30.4)	0.935
	distal	0.356 (0.345, 0.372)	0.689 (0.672, 0.703)	0.526 (0.399, 0.666)	15.5 (13.9, 17.4)	1.21
GCLG−CRP	proximal	0.340 (0.334, 0.346)	0.769 (0.743, 0.790)	0.942 (0.717, 1.20)	27.8 (24.5, 37.8)	1.78
	distal	0.335 (0.328, 0.342)	0.684 (0.653, 0.710)	0.909 (0.716, 1.13)	21.9 (18.0, 28.2)	1.61

[a] Measured in TEK(75) buffer and 150 μM cAMP at pH 7.80 and 25.0 °C. [b] CPM covalently attached to the 5′-end of the strand proximal or distal to the conserved TGTGA motif. [c] Limiting anisotropy of the probe. [d] fxb_2 is the amplitude of the signal due to the contribution of the rotational correlation time ϕ_2 to the overall signal; $fxb_1 + fxb_2 = 1$, where fxb_1 is the amplitude for the rotational correlation time ϕ_1. [e] Rotational correlation time represents the fast, local dynamic motion of the probe. [f] Rotational correlation time that reports on the tumbling motion of the DNA. [g] Reduced χ^2 for the global analysis of the data. [h] Error in parentheses expressed in terms of 67% confidence intervals.

presence of CRP than those parameters are when the protein associates with distally labeled CPM−*GCGG* and CPM−*GCLG*, respectively (Figure 4). In contrast, the phase and modulation ratio of CPM−*LCLL* in the presence of CRP are reduced to the same extent, regardless of the probe's location. This implies that the two ends of the *lac* (*LCLL*) sequence, when bound to CRP, are in similar environments.

Global analysis of the data revealed that two rotational correlation times were observed for CPM−DNA (Table 3). One rotational correlation time, ϕ_1, was very fast, insensitive to the DNA sequence, the probe's location, and CRP binding to DNA. This rotational correlation time is probably reporting on the local, dynamic motion of the fluorophore. The other rotational correlation time of CPM−DNA, ϕ_2, was much shorter than ϕ_1 and reflects the tumbling motion of the DNA in solution. The rotational correlation time ϕ_2 and its amplitude (fxb_2) of CPM−DNA were insensitive to the probe's location and DNA sequence in the absence of CRP. Yet, the magnitude of the rotational correlation time ϕ_2 and its amplitude (fxb_2) of CPM−DNA were observed to increase upon CRP−DNA complex formation. These parameters appear to detect differences in the DNA sequence and probe location (Table 3). The rotational correlation time ϕ_2 and the amplitude (fxb_2) of CPM−*LCLL* in the presence of CRP are the same regardless of the probe's location. As was true for the rotational correlation time ϕ_2 of CPM−*LCLL*−CRP, the rotational correlation time ϕ_2 of the CPM−*GCLG*−CRP complex was essentially the same with the fluorophore located on either end within experimental error (Table 3). Yet, the amplitude (fxb_2) of the proximally labeled *GCLG*−CRP complex increased slightly in the presence of CRP, while the fxb_2 of the distally labeled *GCLG* was insensitive to the presence of CRP. CRP binding to CPM−*GCGG* yielded effects on the fxb_2 parameter similar to those found for CPM−*GCLG*. In contrast, a different trend in the rotational correlation time ϕ_2 was observed for the CPM−*GCGG*−CRP complex relative to those observed for the association of CPM−*GCLG* and CPM−*LCLL* with CRP. The effect of CRP binding to CPM−*GCGG* on the rotational correlation time ϕ_2 was dependent on the location of the probe. The ϕ_2 for the proximally labeled CPM−*GCGG*−CRP complex was similar to those found for the CPM−*GCLG*−CRP complex. Nevertheless, the rotational correlation time ϕ_2 for the proximally labeled CPM−*GCGG*−CRP in the presence of CRP was 25 ns and is greater than the value of 16 ns for ϕ_2 obtained for the distally labeled CPM−*GCGG*−CRP complex.

DISCUSSION

All of the fluorescence methods used in this study consistently show that the symmetry of the CRP-induced DNA bending is sequence dependent. The two ends of the *gal* (*GCGG*) sequence assume different distances from CRP when complexed with CRP, although the bending of the *lac* (*LCLL*) and *GCLG* sequences is symmetric. The induced bending is a function of the sequence in the half-site in conjunction with the flanking sequence. There is ample evidence in the literature to indicate that these fluorescence methods yield quantitatively valid results in the bending geometry of DNA induced by CRP binding (*31*). The geometry of the bent *lac* sequence deduced by these fluorescence approaches is consistent with that observed by X-ray crystallography (*10*), electrophoresis (*8, 9*), and recently by electric dichroism (*32*). Thus, the observed asymmetric bending of the *gal* sequence represents the first example of a deviation in the bending geometry. Furthermore, conclusions derived from these structural studies are consistent with that gleaned from the thermodynamics study (*21*).

The rotational correlation times of CPM−DNA, in the presence of the protein, reflect the tumbling of the macromolecular complex in solution. The theoretical rotational correlation time calculated for a sphere with a mass of 63 000 Da (representing the mass of the protein−DNA complex) is ∼26 ns. The rotational correlation times of CRP bound to CPM−*lac* are 21 ns, and the ratio of ϕ_2 values is 1.0. Thus, these probes located at either end of the DNA reflect the global tumbling motion of the entire complex. This is possible only if the ends of *lac* are bent toward the protein and bent symmetrically. The results from fluorescence dynamics experiments clearly indicated that the environments of the two ends of the *gal* sequence when complexed to CRP are distinctly different from each other, indicating structural asymmetry of the complex. The ratio of ϕ_2 for proximally and distally labeled probes is 1.6. The proximally labeled

end reflects the global tumbling motion of the complex, whereas the other does not. Structural and dynamic asymmetry of the two ends of *gal* in the presence of CRP have not been observed by other methods such as gel electrophoresis (*9*) and DNA footprinting techniques (*16*). The rotational correlation time of the distally labeled CPM−*gal* bound to CRP is much lower than the rotational correlation time expected for a complex with this mass. However, the rotational correlation time is greater than the value observed for free CPM−DNA. Thus, either the probe is reporting on a different tumbling axis, e.g. the probe being further away from the protein molecule, or the probe is only observing a portion of the protein−DNA complex, e.g. the complex between DNA and one subunit of CRP, when the label is attached to the distal end of *gal*. It is interesting to note that the ratio of ϕ_2 values for the hybrid sequence *GCLG* is 1.3, which is between the values of 1.0 and 1.6 for *lac* and *gal*, respectively. This implies that structural dynamic properties of the *GCLG*−CRP complex are truly reporting on a hybrid sequence, and CRP is able to recognize such differences in the sequence (see Table 1 for sequences). Thus, this method is sensitive to monitor small perturbations in the structure of the complex that are caused by protein−DNA complex formation.

The asymmetric nature of binding of *gal* as detected by dynamic fluorescence measurement is consistent with the results of the static energy transfer study. The apparent energy transfer from CRP to the proximally labeled CPM−*GCGG*, −*GCCG*, and −*GCLG* suggests that the probe is closer to the protein when the CRP binding site contains the *gal* background sequence compared to the distance between CRP and proximally labeled CPM−*lac*. This interpretation is consistent with the extensive electrophoretic studies performed on the intrinsic flexibility and protein-induced bendability of A tract sequences within B-DNA (*33*−*38*). The minimum number of A bases in a tract that shows a greater propensity for intrinsic bending is 4 bp (*37*, *39*). An A tract exists in the *gal* sequence (AAAAG) and is proximal to the TGTGA motif (see Table 1). Thus, the fluorescence results are consistent with these well-established and extensive studies on DNA bending properties (*3*, *5*, *18*, *40*, *41*). Nevertheless, the same explanation cannot be invoked to explain the fluorescence results of the distally labeled CPM−*gal* in the presence of CRP. Another (pseudo) A tract is observed in the *gal* sequence and includes the inverted repeat region, AATAAATT (inverted repeat is underlined). It is known that disrupting an A tract with another base reduces the intrinsic flexibility of the sequence, although a T substitution for an A in the tract produces a less deleterious effect on the A tract properties than a cytosine or guanine substitution (*42*, *43*). On the basis of this knowledge, one would expect that the DNA structure in this region of *gal* would be more facile for CRP to deform. Our results suggest that this rationale employed here is too simplistic. The probe located on the distal end of *gal* in the presence of the protein is further away from the protein than when the probe is located on the proximal end of *gal*.

Other electrophoretic studies using CRP and DNA sequences that contain the *lac* and *icap* recognition motifs embedded in various flanking sequences demonstrate that the base sequence at positions −10 and −11 can influence the degree of mobility of the DNA through the gel.[4] A comparison of the *lac* and *gal* sequences at positions −10 and −11 with the results obtained from Gartenberg and Crothers (*30*) ranking of bases with respect to their migration rate, which is related to their degree of "bendability", shows that the *lac* bases at this position favor the CRP-induced bend toward the protein. Their study also predicts that the *gal* sequences at positions −10 and −11 also have a high probability of bendability. In contrast, one would predict, on the basis of the previous electrophoretic results, that the bases located at positions 10 and 11 in the *gal*−CRP binding site are not as prone to protein-induced deformation, relative to the sequences corresponding to the analogous position in the *lac*−CRP binding site. The fluorescence results presented here qualitatively agree with the previous results obtained from electrophoretic studies. However, the effects of specific bases located at positions 10 and 11 must be viewed in the context of the adjacent sequence. Let us review the results for the *gal* and *GCLG* sequences. The bending of the *gal* sequence is asymmetric with the end proximal to the ATAAA half-site bending less (see Table 1 for sequences). The bending of the *GCLG* sequence is more symmetric. The bases at positions 10 and 11 in both sequences are the same. The only differences in sequence are located in the half-site: ATAAA versus TCACT. Thus, the sequence in the half-site in conjunction with flanking sequence defines the geometry of the bent DNA.

The conclusion that the binding of the *gal* sequence is asymmetric is also consistent with the thermodynamic data in the preceding paper (*21*). While the inclusion of both half-sites for *lac* shows a significantly greater affinity for CRP, there is no enhancement in affinity when both half-sites of *gal* are present. When CRP binds to the *lac* sequence, it induces a symmetrical bend in the DNA. The CRP-induced bend in the DNA increases favorable contacts between CRP and DNA. These favorable structural changes are reflected in the high affinity of CRP for the *lac* sequence. In contrast, the *gal*−CRP complex is structurally asymmetric, and one of the half-sites (the inverted repeat) must not be making maximum contacts with CRP. As a result, the affinity of CRP for *gal* is weaker. The difference in the change in free energy of the half-sites of the *lac*−CRP complex relative to that of the *gal*−CRP complex is −2.4 ± 0.7 kcal/mol ($\Delta\Delta G_i$ in ref *21*). Thus, both thermodynamic and structural data reveal a consistent view of a difference in the mode of interaction between CRP and *gal* or *lac* sequences.

The differences in the dynamics of DNA−CRP interactions, observed by using fluorescence methods, may be detecting inherent differences in the molecular mechanism of CRP on class I and class II CRP binding sites. For the *gal* operon, RNA polymerase has two overlapping promoter sites, P1 and P2. In the absence of CRP, there is only a small energetic advantage for RNA polymerase binding to P1 over binding to the P2 site (−0.4 kcal/mol; *44*). Two different mechanisms have been proposed for the transcrip-

[4] The numbering of the DNA sequences is the same used by Gartenberg and Crothers (*30*). Briefly, the dyad axis is the reference point (position zero). Integers represent the position of the bases in the sequence relative to the dyad axis. Positive and negative numbers refer to nucleotides to the right- and left-hand side of the axis when the sequences are aligned by the conserved TGTGA motifs.

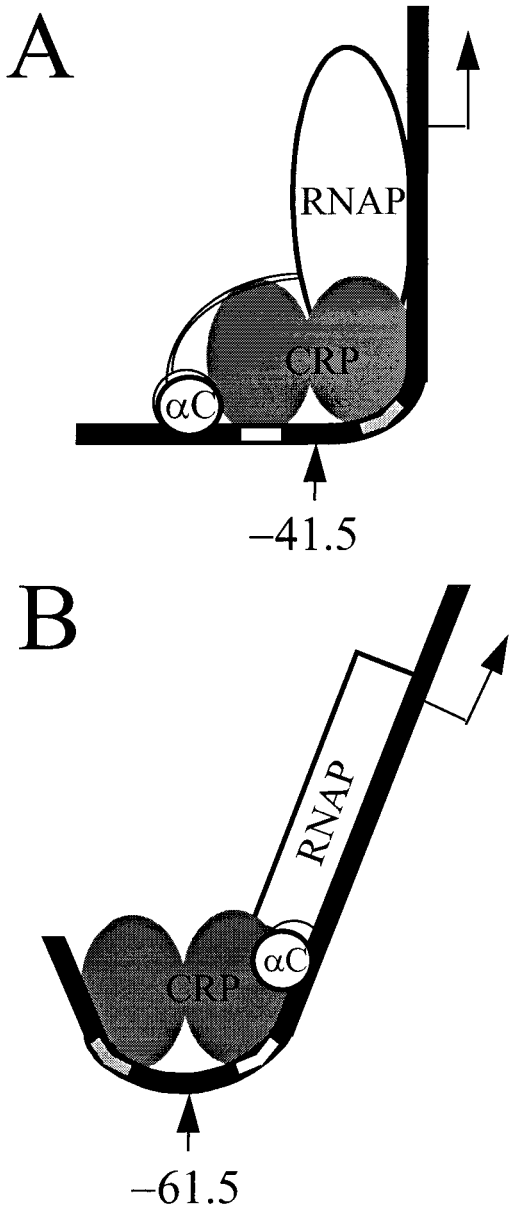

FIGURE 5: Models depicting the geometry of the DNA bend in class I (*lac* operon) and class II (*gal* operon) CRP binding sites. RNAP represents all the subunits of RNA polymerase. αC denotes the C-terminal domain of the α subunits of RNA polymerase. Arrows represent the direction of transcription. The conserved TGTGA and inverted repeat sequences are shown in dark gray and white regions, respectively, embedded in the DNA strand. (A) Asymmetric bending of the DNA in the *gal* operon (class II). A larger deformation in the DNA occurs proximal to the conserved TGTGA motif. (B) Symmetric bending of the DNA in the *lac* operon (class I).

tion of P1 and P2 sites on DNA. In both cases, transcription is regulated by the CRP−DNA interaction. Transcription from P2 occurs readily in the absence of CRP, but when CRP binds to the *gal* P1−CRP binding site on DNA, it represses transcription from P2 and induces RNA polymerase to bind >99% to the P1 site, which activates transcription from P1 (*44*). The binding of CRP and RNA polymerase to *gal* is cooperative in nature. Previous work by Zhou and co-workers (*13*) demonstrates that the C-terminal domain of the α subunit of RNA polymerase makes contact with the DNA upstream from the *gal* P1−CRP binding site. The asymmetry in the CRP-induced bend in DNA demonstrated in this work not only may provide the structural requirements for RNA polymerase to contact the DNA sequence upstream from the *gal* P1−CRP binding site but also may act as an allosteric effector, thus supplying RNA polymerase the information necessary for it to transcribe the S1 mRNA transcript. Figure 5A depicts a model that shows the asymmetric bend induced by *gal*−CRP complex formation. The C-terminal domain of the α subunit of RNA polymerase has been shown to contact CRP and DNA in a region that is distally located from the conserved TGTGA motif in the CRP binding site. In contrast, the mechanism of CRP activation of class I CRP binding sites (*lac* operon) requires a different set of contacts between the DNA and RNA polymerase for transcriptional activity. The symmetrical bend induced by CRP binding in the *lac* P1−CRP binding site (*10*, *11*) results in a different set of contacts between the *lac*, CRP, and RNA polymerase (*45*), as shown in Figure 5B. The C-terminal domain of the α subunit of RNA polymerase binds distally to the conserved TGTGA motif in the *lac*−CRP binding site. The distinct structural dynamics of the two classes of CRP binding sites complexed to CRP act as two different allosteric effectors for RNA polymerase binding to DNA. Therefore, the specific DNA sequences are responsible for the different set of contacts made between these two proteins and DNA and also supply the necessary information for RNA polymerase to be able to distinguish between the two classes of CRP binding sites.

ACKNOWLEDGMENT

The experiments and analyses of the fluorescence data were performed at the Laboratory for Fluorescence Dynamics (LFD) at the University of Illinois at Urbana−Champaign (UIUC). We thank Dr. Theodore L. Hazlett at the Laboratory for Fluorescence Dynamics for his expertise.

REFERENCES

1. Heyduk, T., and Lee, J. C. (1990) *Proc. Natl. Acad. Sci. U.S.A. 87*, 1744−1748.
2. Pyles, E. A., and Lee, J. C. (1996) *Biochemistry 35*, 1162−1172.
3. Perez-Martin, J., Rojo, F., and de Lorenzo, V. (1994) *Microbiol. Rev. 58*, 268−290.
4. Mathews, K. S. (1992) *Microbiol. Rev. 56*, 123−136.
5. Schleif, R. (1992) *Annu. Rev. Biochem. 61*, 199−223.
6. Hagerman, P. J. (1988) *Annu. Rev. Biophys. Biophys. Chem. 17*, 265−286.
7. Liu-Johnson, H.-N., Gartenberg, M. R., and Crothers, D. M. (1986) *Cell 47*, 995−1005.
8. Fried, M. G., and Crothers, D. M. (1983) *Nucleic Acids Res. 11*, 141−158.
9. Wu, H.-M., and Crothers, D. M. (1984) *Nature 308*, 509−513.
10. Schultz, S. C., Shields, G. C., and Steitz, T. A. (1991) *Science 253*, 1001−1007.
11. Heyduk, T., and Lee, J. C. (1992) *Biochemistry 31*, 5165−5171.
12. Zhou, Y., Merkel, T. J., and Ebright, R. H. (1994) *J. Mol. Biol. 243*, 603−610.
13. Zhou, Y., Pendergast, P. S., Bell, A., Williams, R., Busby, S., and Ebright, R. H. (1994) *EMBO J. 13*, 4549−4557.
14. Busby, S., and Ebright, R. H. (1997) *Mol. Microbiol. 23*, 853−859.
15. Schmitz, A. (1981) *Nucleic Acid Res. 9*, 277−292.
16. Taniguichi, T., O'Neill, M., and de Crombrugghe, B. (1979) *Proc. Natl. Acad. Sci. U.S.A. 10*, 5090−5094.

17. Shanblatt, S. H., and Revzin, A. (1987) *J. Biol. Chem. 262*, 11422−11427.
18. Ebright, R. H. (1993) *Mol. Microbiol. 8*, 797−802.
19. Richet, E., and Sogaard-Andersen, L. (1994) *EMBO J. 13*, 4558−4567.
20. Niu, W., Zhou, Y., Dong, Q., Ebright, Y. W., and Ebright, R. H. (1994) *J. Mol. Biol. 243*, 595−602.
21. Pyles, E. A., Chin, A. J., and Lee, J. C. (1998) *Biochemistry 37*, 5194−5200.
22. Lakowicz, J. R. (1983) in *Principles of Fluorescence Spectroscopy*, p 87, Plenum Press, New York.
23. Lakowicz, J. R. (1983) in *Principles of Fluorescence Spectroscopy*, p 131, Plenum Press, New York.
24. Fairclough, R. H., and Cantor, C. R. (1978) *Methods Enzymol. 28*, 347−379.
25. Stryer, L. (1978) *Annu. Rev. Biochem. 47*, 819−846.
26. Bane Hastie, S. (1989) *Biochemistry 28*, 7753−7760.
27. Lakowicz, J. R. (1983) in *Principles of Fluorescence Spectroscopy*, p 15, Plenum Press, New York.
28. Förster, T. (1959) *Discuss. Faraday Soc. 27*, 7−17.
29. Sippel, T. O. (1981) *J. Histochem. Cytochem. 29*, 1377−1381.
30. Gartenberg, M. R., and Crothers, D. M. (1988) *Nature 333*, 824−829.
31. Kolb, A., Busby, S., Buch, H., Garges, S., and Adhya, S. (1993) *Annu. Rev. Biochem. 62*, 749−795.
32. Meyer-Almes, F.-J., and Proschke, D. (1997) *J. Mol. Biol. 269*, 842−850.
33. Trifonov, E. N., and Sussman, J. L. (1980) *Proc. Natl. Acad. Sci. U.S.A. 77*, 3816−3820.
34. Hagerman, P. J. (1985) *Biochemistry 24*, 7033−7037.
35. Koo, H. S., and Crothers, D. M. (1988) *Proc. Natl. Acad. Sci. U.S.A. 85*, 1763−1767.
36. Crothers, D. M., and Drak, J. (1992) *Methods Enzymol. 212*, 46−71.
37. Crothers, D. M., Haran, T. E., and Nadeau, J. G. (1990) *J. Biol. Chem. 265*, 7093−7096.
38. Haran, T. E., Kahn, J. D., and Crothers, D. M. (1994) *J. Mol. Biol. 244*, 135−143.
39. Crothers, D. M. (1994) *Science 266*, 1819−1820.
40. Harrington, R. E. (1993) *Electrophoresis 14*, 732−746.
41. Harrington, R. E. (1992) *Mol. Microbiol. 6*, 2549−2555.
42. Koo, H. S., Wu, H.-M., and Crothers, D. M. (1986) *Nature 320*, 501−506.
43. Hagerman, P. J. (1986) *Nature 321*, 449−450.
44. Dalma-Weiszhausz, D. D., and Brenowitz, M. (1996) *Biochemistry 35*, 3735−3745.
45. Zhou, Y., Busby, S., and Ebright, R. (1993) *Cell 73*, 375−379.

BI972451A